Optically detected magnetic resonance investigation of oxygen luminescence centres in BaF_2

2002 J. Phys.: Condens. Matter 14 6949

(http://iopscience.iop.org/0953-8984/14/28/306)

INSTITUTE OF PHYSICS PUBLISHING JOURNAL OF PHYSICS: CONDENSED MATTER

J. Phys.: Condens. Matter **14** (2002) 6949–6956 PII: S0953-8984(02)36423-3

Optically detected magnetic resonance investigation of oxygen luminescence centres in BaF_2

U Rogulis[1], S Schweizer[2] and J-M Spaeth

Universität Paderborn, Fachbereich Physik, Warburger Str. 100, D-33098 Paderborn, Germany

E-mail: schweizer@physik.upb.de

Received 1 May 2002
Published 5 July 2002
Online at stacks.iop.org/JPhysCM/14/6949

Abstract

The structure of two oxygen-related luminescence centres in oxygen-doped BaF_2 was investigated by means of photoluminescence (PL) and photoluminescence-detected electron paramagnetic resonance (PL-EPR). One of the oxygen-related luminescences peaking at 2.83 eV is associated with an excited triplet state ($S = 1$) of an oxygen–vacancy complex with the z-axis of the fine-structure tensor parallel to the $\langle 110 \rangle$ direction. This complex can be described as an oxygen on a fluorine lattice site with a *next-nearest* fluorine vacancy along the $\langle 110 \rangle$ direction. The luminescence at 2.25 eV is also associated with a triplet state. Its PL-EPR spectrum is probably due to oxygen–vacancy complexes with a *nearest* fluorine vacancy along the $\langle 100 \rangle$ direction.

1. Introduction

Barium fluoride is one of the most important high-density luminescent materials used for γ-ray and elementary particle detection. However, the incorporation of oxygen affects the performance of this scintillator seriously [1]. It has already been discussed in [2] that oxygen may be incorporated in BaF_2 as oxygen–vacancy dipoles and as aggregates of such dipoles. Nevertheless, a structure-sensitive investigation on the oxygen-related luminescence centres has not yet been done. In order to get structural information on these centres we detected the electron paramagnetic resonance-induced changes in the photoluminescence (PL). This technique, which is usually called photoluminescence-detected electron paramagnetic resonance (PL-EPR), has already been used for investigations of the oxygen–vacancy complexes in BaFBr [3] and BaFCl [4].

[1] Permanent address: Institute of Solid State Physics, University of Latvia, LV-1063 Riga, Latvia.
[2] Author to whom any correspondence should be addressed.

0953-8984/02/286949+08$30.00

2. Experiment

2.1. Sample preparation

BaF_2 crystals were grown in graphite crucibles with the Bridgman method from a mixture of BaF_2 and 10 000 ppm BaO. It seems from the luminescence intensity that only a very small fraction of oxygen is incorporated in the lattice. BaF_2 crystallizes in cubic symmetry with the atoms of its four molecules per unit cell in the O_h^5 ($Fm3m$) positions [5]. BaF_2 single crystals can be cleaved parallel to the {111} planes. Prior to the measurements the crystals were annealed for 1 h at 500 °C in air and afterwards quenched to RT.

2.2. Spectroscopy

Luminescence and luminescence excitation spectra were measured with a single-beam spectrometer in which 0.25 m double monochromators (Spex) were available for excitation and luminescence. The excitation was carried out with a deuterium lamp; the PL was detected using single-photon counting with a photomultiplier. The spectra were not corrected for the spectral sensitivity of the experimental set-up.

PL-EPR spectra were recorded at 1.5 K with a custom-built, computer-controlled spectrometer working at 25 GHz (K band). The samples were excited in the ultraviolet (UV) spectral range with a deuterium lamp and subsequent interference filters in the range between 210 and 300 nm. PL was detected by a photomultiplier in the spectral range between 380 and 800 nm using edge filters. The microwave modulation frequency was between 80 Hz and 5 kHz; the EPR angular dependence was recorded for a microwave modulation frequency of 270 Hz.

3. Experimental results

3.1. Photoluminescence

The UV-excited luminescence band of oxygen-doped BaF_2, recorded at RT, peaks at 2.29 eV (541 nm) (figure 1(a), curve 1). The corresponding excitation band peaking at 4.56 eV (272 nm) is shown in figure 1(b), curve 2.

At 10 K the luminescence spectra show several overlapping luminescence peaks (figure 1(b), curves 1 and 2). For an excitation energy of 4.77 eV (260 nm) the spectrum peaks at 2.25 eV (550 nm) (see figure 1(b), curve 1), whereas for 5.64 eV (220 nm) the PL spectrum comprises two peaks at 2.55 eV (486 nm) and 2.83 eV (438 nm), respectively (see figure 1(b), curve 2). The PL excitation spectra, detected in the 2.25 and 2.83 eV luminescence bands, are shown in figure 1(b), curves 3 and 4, respectively.

PL and PL excitation, recorded at 80 K, yielded the same spectral characteristics as at 10 K.

3.2. Photoluminescence-detected EPR

The ground state of an O^{2-} impurity is diamagnetic and can thus not be detected by means of EPR. However, the excited state of O^{2-} can become paramagnetic if the excited electron and the remaining unpaired electron have parallel spins, i.e. if the excited $(O^{2-})^*$ is in a triplet state [3, 4].

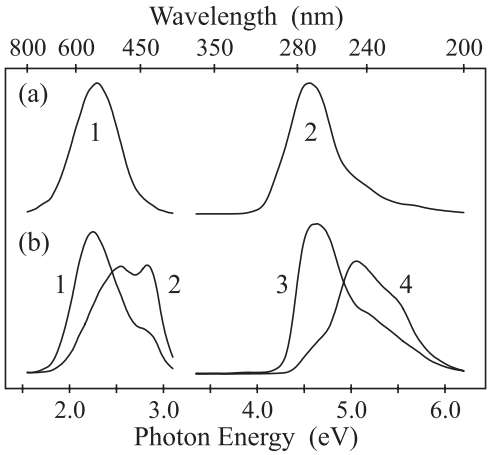

Figure 1. Luminescence and excitation spectra of oxygen-doped BaF_2. (a) PL, excited at 4.56 eV (curve 1), and PL excitation, detected at 2.29 eV (curve 2). The spectra were recorded at RT. (b) PL, excited at 4.77 eV (curve 1) and 5.64 eV (curve 2), and PL excitation spectra, detected at 2.25 eV (curve 3) and 2.83 eV (curve 4). The spectra were recorded at 10 K.

3.2.1. Luminescence centre I. Figure 2 shows a PL-EPR spectrum of oxygen-doped BaF_2 in the K band (25.60 GHz) for a magnetic field orientation in the (110) plane at an angle of approximately 40° with respect to the [001] axis. The PL was excited at 1.5 K with a 240 nm interference filter and detected in the integral luminescence with a 380 nm edge filter. The angular dependence of these lines for a rotation of the magnetic field in the (110) plane is presented in figure 3. We used the spin Hamiltonian of a triplet spin ($S = 1$) system with an orthorhombic fine-structure (FS) tensor to analyse the angular dependence of the PL-EPR lines:

$$\mathcal{H} = \mu_B \vec{B} \cdot \underline{\underline{g}} \cdot \vec{S} + \vec{S} \cdot \underline{\underline{D}} \cdot \vec{S} \tag{1}$$

where $\underline{\underline{g}}$ and $\underline{\underline{D}}$ are the g-and D-tensor, respectively. μ_B is the Bohr magneton, $\vec{B}$ is the magnetic field vector and $\vec{S}$ is the electron spin operator. The orientations of the g- and D-tensors can be described with a set of Euler angles. In the principal axes system the g-tensor is characterized by its three principal values g_{xx}, g_{yy} and g_{zz}. The D-tensor can be expressed using the two FS values D and E in the principal axes system, which have the usual meaning as the axial ($D = \frac{3}{2}D_{zz}$) and non-axial ($E = \frac{1}{2}(D_{xx} - D_{yy})$) parts, respectively (see e.g. [6]). The calculated EPR angular dependence is shown in figure 3 by solid curves. The spin Hamiltonian parameters used are collected in table 1. The resonances in the magnetic field range between 400 and 1700 mT are due to 'allowed' ($\Delta m_S = \pm 1$) transitions whereas the resonances between 150 and 300 mT are associated with 'forbidden' ($\Delta m_S = \pm 2$) ones. Surprisingly, they have larger intensities than the 'allowed' ones. The principal axes (z) of the g- and the D-tensor are collinear and aligned along a $\langle 110 \rangle$ direction.

A triplet spin system having orthorhombic symmetry with the principal axis z along a $\langle 110 \rangle$ direction should have six magnetically non-equivalent centre orientations. The spectrum of each centre orientation should be split by the FS interaction into two lines which are symmetrical about the g-factor. The largest splitting is for $\vec{B} \parallel \langle 110 \rangle$. However, for a rotation of the magnetic field in a $\{110\}$ plane the angular dependence shows only four different centre orientations of which two consist of two magnetically equivalent orientations.

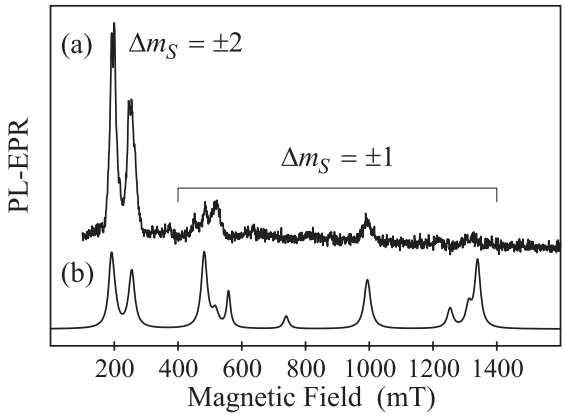

Figure 2. (a) A PL-EPR spectrum of oxygen-doped BaF_2 for an orientation of the magnetic field in the (110) plane at an angle of approximately 40° with respect to [001]. The spectrum was recorded as microwave-induced changes in the integral PL at 1.5 K applying a microwave frequency of 25.60 GHz. The PL was excited with a 240 nm interference filter and detected in the integral luminescence with a 380 nm edge filter. (b) The EPR spectrum calculated using the parameters for luminescence centre I.

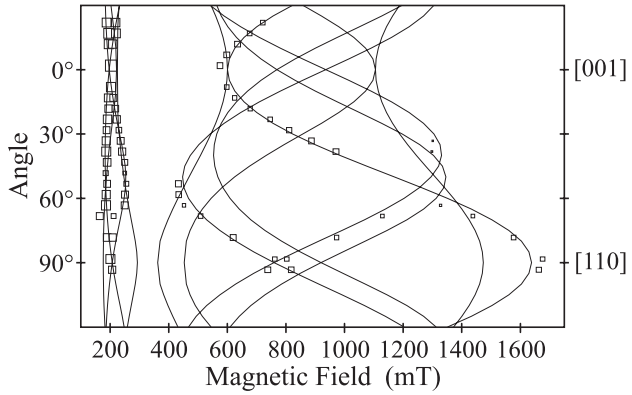

Figure 3. The angular dependence of the PL-EPR lines, recorded for a rotation of the magnetic field in the (110) plane. The PL was excited with a 240 nm interference filter and detected in the integral luminescence with a 380 nm edge filter. The open squares represent the experimental line position; the solid curves were calculated by using the FS parameters of table 1.

Table 1. Parameters of the spin Hamiltonian (equation (1)) for oxygen-related luminescence centres in BaF_2. For the luminescence centre I the z-axes of the g- and the D-tensor are parallel to a $\langle 110 \rangle$ direction. The z-axis of the D-tensor of the luminescence centre II is assumed to be parallel to a $\langle 100 \rangle$ direction; the g-value is set to $g = 2.00$. For centre I the precision for g is ± 0.02.

Centre	g_{xx}	g_{yy}	g_{zz}	$\lvert D/g_e\beta_e \rvert$ (mT)	$\lvert E/g_e\beta_e \rvert$ (mT)
I	1.89	1.86	1.97	708 ± 5	95 ± 5
II		$g = 2.00$		870	(87)

The largest PL-EPR line intensity of the luminescence centre I was obtained at a photon energy of 2.83 eV (438 nm) which is one of the maxima of the luminescence spectrum shown

in figure 1(b), curve 2. On setting the edge filters to energy lower than 2.83 eV, the PL-EPR line intensity decreases. Thus, it is thought that the peak at 2.55 eV is not related to a triplet system. The best excitation energy was found to be at approximately 5.17 eV (240 nm), which is in agreement with the excitation spectrum depicted in figure 1(b), curve 4.

Attempts to determine the sign of the FS parameter D by measuring the magnetic circular polarization of the emission (MCPE) failed. The calculated EPR line intensities (figure 2(b)) show that the large FS parameters of luminescence centre I lead to comparable values of the transition probabilities of the 'allowed' and 'forbidden' transitions. For such large FS parameters the Zeeman levels at the applied magnetic field cannot be considered any longer as pure $m_S = -1, 0, +1$ states. Since the observed line intensities of the 'forbidden' transitions are much larger than the 'allowed' ones, which cannot be explained by FS mixing of the states, they are obviously influenced by dynamical effects such as the radiative lifetimes of the different Zeeman levels. The spin–lattice relaxation times are rather long. The PL-EPR line intensity decreased to half its value on changing the microwave modulation frequency from 270 Hz to 1.5 kHz and vanished for 5 kHz indicating that the spin–lattice relaxation times are longer than several tenths of a ms.

Time-resolved PL-EPR measurements (figure 4) were carried out by monitoring the time evolution of the luminescence intensity after switching resonant microwaves on and off [3, 7]. After switching on resonant microwaves between the $m_S = \pm 1$ states a steep rise in the luminescence intensity is observed which decays after about 4 ms, while after switching off the microwaves there is a decrease in the luminescence intensity, again reaching its steady state after about 6 ms. The time evolution of the PL-EPR signal can be analysed by means of rate equations under the assumption that the spin–lattice relaxation time is long compared to the radiative lifetimes of the triplet states [7]. After the microwave-induced transition between two levels i and j (i, j: $m_S = \pm 1$) has been switched off at the time t_0, the time evolution of the luminescence intensity can be described by

$$\Delta I(t) \propto \frac{k_i^{\mathrm{rad}}}{k_i} \exp(-k_i(t - t_0)) - \frac{k_j^{\mathrm{rad}}}{k_j} \exp(-k_j(t - t_0)) \tag{2}$$

where: $\Delta I(t)$ is the change in luminescence intensity; k_i and k_j are the total probabilities of decay to the ground state of the triplet levels i and j which were connected with a microwave transition before the microwaves were switched off; and k_i^{rad} and k_j^{rad} are the radiative parts of the (total) decay rates without microwaves [7]. The time evolution shown in figure 4 could be simulated by assuming two decay times $\tau_i = k_i^{-1} = (0.17 \pm 0.02)$ ms and $\tau_j = k_j^{-1} = (2.1 \pm 0.2)$ ms and the ratio $(k_i^{\mathrm{rad}}/k_i)/(k_j^{\mathrm{rad}}/k_j)$ of the two amplitudes to be equal to 1.5 ± 0.1. The large line intensity of the 'forbidden' transitions is obviously due to the fact that the two decay times of the $m_S = \pm 1$ states differ by more than an order of magnitude.

A similar time-resolved measurement and analysis of the 'allowed' transitions was not possible due to their low signal-to-noise ratio. Therefore we cannot say anything about $\tau_{m_S=0}$.

3.2.2. Luminescence centre II. Further PL-EPR lines at lower fields compared to those for figures 2 and 3 could be detected at 2.25 eV (550 nm) which is the maximum of the luminescence spectrum of figure 1(b), curve 1. The best excitation energy of 4.59 eV (270 nm) is in agreement with the excitation spectrum shown in figure 1(b), curve 3. The resonances are in the magnetic field range between 0 and 150 mT as shown in figure 5(a). They are almost angle independent and are attributed to 'forbidden' transitions of a similar triplet system with larger FS parameters than those of the ⟨110⟩-oriented luminescence centres (luminescence centre I). Unfortunately, we could not detect any 'allowed' transitions and a complete analysis was thus not possible. As will be discussed later, we assign the luminescence centre I to an oxygen–

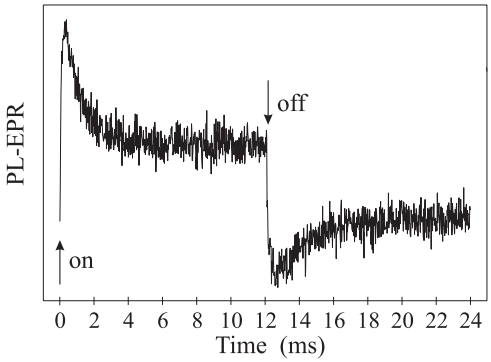

Figure 4. Time-resolved PL-EPR measurements, recorded in the 'forbidden' transitions for $\vec{B} \parallel [001]$ at 1.5 K. The PL was excited with a 240 nm interference filter and detected in the integral luminescence with a 380 nm edge filter. The microwaves were switched on at $t = 0$ ms and switched off at $t = 12$ ms.

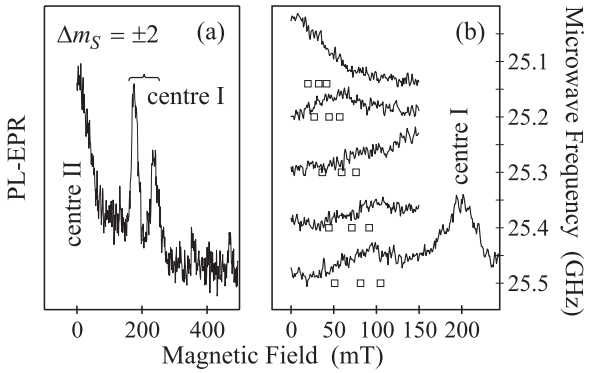

Figure 5. (a) A PL-EPR spectrum of oxygen-doped BaF_2 for an orientation of the magnetic field in the (110) plane with an angle of approximately 60° with respect to [001]. The spectrum was recorded as microwave-induced changes in the integral PL at 1.5 K applying a microwave frequency of 25.16 GHz. The PL was excited with a 270 nm interference filter and detected in the integral luminescence with a 370 nm edge filter. (b) The microwave frequency dependence of the PL-EPR spectra of centre II for $\vec{B} \parallel [001]$. The open squares represent the theoretical line positions calculated by using the FS parameters of table 1.

vacancy complex with a *next-nearest* fluorine vacancy along a ⟨110⟩ direction. Since the FS parameters of the luminescence centre II are obviously larger than those of the luminescence centre I, we tentatively assign the corresponding resonances to an oxygen–vacancy complex with a *nearest* fluorine vacancy along a ⟨100⟩ direction. Figure 5(b) shows the microwave frequency dependence of the 'forbidden' transitions of the luminescence centre II in the small frequency range available in our K-band spectrometer. Since the 'forbidden' resonances are near to zero field, they are very sensitive to microwave frequency changes. This microwave frequency dependence can be analysed and gives a rough estimate for the FS parameters. For the simulation the parameters listed in table 1 were used. We assumed that $g = 2.00$ and that the z-axis of the D-tensor is parallel to a ⟨100⟩ direction and the non-axial part E of the FS tensor is 10% of the axial part D. This E/D ratio of at least 10% seems to be characteristic for oxygen–vacancy complex centres [3, 4].

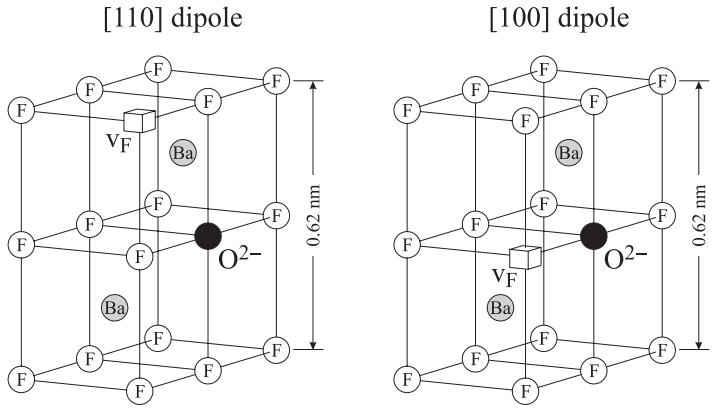

Figure 6. Models of the O^{2-}–v_F dipoles in cubic BaF_2.

4. Discussion

The PL spectra of oxygen-doped BaF_2 (figure 1, curves 1 and 2) comprise at least three different luminescence bands of which two could be associated with two different triplet states formed after exciting O_F^{2-}. As for BaFBr and BaFCl it is assumed that the oxygen 2p electron is transferred to a nearby F^- vacancy but remains strongly coupled to the remaining oxygen 2p hole resulting in parallel spins, i.e. a triplet state. A F^- vacancy is needed for charge compensation of O_F^{2-} [3, 4]. The FS tensor D can be interpreted by calculating the spin–spin interaction for this model.

The zero-field splitting parameter D consists of the two parts D_{ss} and D_{so}, where D_{ss} is due to the spin–spin interaction and D_{so} due to the spin–orbit interaction [8]. In [3, 4] it has already been estimated that the latter is probably very small and can thus be neglected, similarly to the case for the STEs in alkali fluorides [9]. In analogy to the situation in BaFBr and BaFCl [3, 4], the optically excited oxygen 2p electron is transferred to an s-like state centred on a nearby F^- vacancy (v_F). The 2p orbital of the remaining oxygen hole is directed parallel to the O_F^-–v_F connecting line. The axial part D_{ss} of the FS D-tensor was estimated by assuming Gaussians, i.e., $\exp(-\alpha r^2)$, for the wavefunctions of the electron at the F^- vacancy (F centre) and the p hole of the oxygen on the fluorine site and by calculating the dipole–dipole interaction between them [3, 4]. For the oxygen 2p hole we assumed that $\alpha_{\text{hole}} = 0.3$ au^{-2} [3, 4] while for the s electron of the F centre, α_{electron} was varied.

Assuming an unperturbed lattice for the luminescence II, i.e., a distance of 0.310 nm between the oxygen 2p hole and the s electron on the *nearest* F^- vacancy in the $\langle 100 \rangle$ direction, the measured FS parameter D could be understood by using $\alpha_{\text{hole}} = 0.3$ au^{-2} and $\alpha_{\text{electron}} = 0.05$ au^{-2} (see figure 6 and table 2). Taking the same values for α_{hole} and α_{electron}, the measured FS parameter D of the luminescence centre I would require a smaller distance (0.352 nm) as compared to the unperturbed lattice (0.438 nm) between the oxygen 2p hole on the fluorine site and the s electron on the *next-nearest* F^- vacancy (see figure 6 and table 2), i.e., an inward relaxation by 20% compared to the ordinary lattice. A value of α_{electron} larger than 0.05 would hardly increase D for the $\langle 110 \rangle$ complex (e.g. $\alpha_{\text{electron}} = 0.1$, $D = -475$ mT), while the D-value for the $\langle 100 \rangle$ complex would become too large. Thus, we conclude from our analysis that a lattice relaxation of the $\langle 110 \rangle$ complex occurs. Whether it is 20% as estimated or somewhat less we cannot say, in view of the rather crude model used to calculate D.

Table 2. Theoretical values for the axial part D of the FS interaction calculated for different distances. For the calculations, $\alpha_{\text{hole}} = 0.3$ au^{-2} and $\alpha_{\text{electron}} = 0.05$ au^{-2} were used.

d (au)	d (nm)	D_{theo} (mT)	Complex
5.86	0.310	−861	⟨100⟩, usual separation
6.65	0.352	−708	⟨110⟩, inward relaxation by 20%
8.28	0.438	−439	⟨110⟩, usual separation

5. Conclusions

PL-EPR yielded new information about two different excited triplet states of oxygen-related luminescence centres in BaF_2:O crystals.

The luminescence band at 2.83 eV (for an excitation energy of 5.17 eV) is due to an oxygen–vacancy complex with an oxygen on a fluorine site with a *next-nearest* fluorine vacancy along a ⟨110⟩ direction.

The luminescence band at 2.25 eV is probably associated with oxygen–vacancy complexes with a *nearest* fluorine vacancy along a ⟨100⟩ direction.

Acknowledgment

The authors would like to thank Professor Dr K S Song for providing the code for the calculation of the FS parameters.

References

[1] Vail J-M, Emberly E, Lu T, Gu M and Pandey R 1998 *Phys. Rev.* B **57** 764
[2] Radzhabov E and Figura P 1994 *Phys. Status Solidi* b **186** K37
[3] Koschnick F-K, Hangleiter Th, Song K S and Spaeth J-M 1995 *J. Phys.: Condens. Matter* **7** 6925
[4] Schweizer S, Rogulis U, Song K S and Spaeth J-M 2000 *J. Phys.: Condens. Matter* **12** 6237
[5] Wyckoff R W G 1964 *Crystal Structures* vol 1 (New York: Interscience)
[6] Spaeth J-M, Niklas J R and Bartram R H 1992 *Structural Analysis of Point Defects in Solids (Springer Series in Solid State Sciences vol 43)* (Berlin: Springer)
[7] Chan I Y 1982 *Triplet State ODMR Spectroscopy* ed R H Clark (New York: Wiley) ch 1
[8] Song K S and Williams R T 1993 *Self-Trapped Excitons (Springer Series in Solid-State Sciences vol 105)* (Berlin: Springer) ch 5
[9] Song K S, Leung C H and Spaeth J M 1990 *J. Phys.: Condens. Matter* **2** 6373